Sun Vector Based Attitude Determination of Passively Magnetically Stabilized Spacecraft

Anton H.J. de Ruiter[1] and Long Tran[2]
Ryerson University, 350 Victoria Street, Toronto, ON, Canada M5B 2K3

Balaji Shankar Kumar[3] and Andriy Muntyanov[4]
exactEarth Ltd., 60 Struck Court. Cambridge, ON, Canada N1R 8L2

This paper examines the problem of attitude estimation for passively magnetically stabilized spacecraft using only sun vector measurements. An analytical investigation of local observability is performed in the case where the spacecraft magnetic dipole is constant. This is relevant, since for passively stabilized spacecraft using permanent magnets and magnetic hysteresis rods, the hysteresis rod dipole moments are nearly constant at steady-state. It is shown that under reasonable assumptions on the Earth's magnetic field, not only are the attitude and angular velocity locally observable, but if one component of the magnetic dipole moment is known, then the remaining two components of the magnetic dipole moment are locally observable also. Numerical examples of three attitude estimation schemes are presented, demonstrating successful state estimation of passively magnetically stabilized spacecraft.

I. Introduction

The attitude determination capability is an essential component for most spacecraft attitude control systems. As such, there has been and continues to be extensive research performed on spacecraft attitude determination. A number of different types of attitude sensors provide vector

---

[1] Associate Professor, Department of Aerospace Engineering; aderuiter@ryerson.ca.
[2] M.A.Sc Candidate, Department of Aerospace Engineering; ldtran@ryerson.ca.
[3] Senior Mission Systems Engineer, Systems Engineering and Applied Research; Balaji.Kumar@exactearth.com.
[4] Satellite Operations Engineering Associate, Operations; Andriy.Muntyanov@exactearth.com.

measurements. Sun-sensors provide sun-vector measurements, three-axis magnetometers provide measurements of the Earth's magnetic field vector, and star trackers are based upon the measurement of star pointing vectors. As such, several researchers have developed spacecraft attitude estimation schemes utilizing vector measurements, including stochastic estimators [1, 2] and deterministic observers [3, 4]. A comprehensive survey of spacecraft attitude estimation methods may be found in [5].

The ability to estimate a spacecraft's attitude using only a single vector measurement is useful for situations when attitude sensors fail leaving only a single vector measurement, or on very small satellites which are not equipped with a number of attitude sensors. For example, [6] presents a real flight example where attitude is determined for a magnetically passively stabilized nanosatellite using only measurements of solar panel currents. The solar panel currents are pre-processed to obtain a sun-vector, which is then used within a multiplicative extended Kalman filter (MEKF) to estimate attitude and angular velocity.

Various authors have investigated both spacecraft attitude and angular velocity determination using a single vector measurement. In some cases, the vector measurement is augmented with a gyro which provides an angular velocity measurement [7, 8]. In other cases, the vector measurement is used alone [9, 10]. As is well known (and is demonstrated in Section III A of this paper for completeness), the attitude for a torque-free spacecraft is not observable when the single vector measurement is inertially fixed. Therefore, in all of these cases, observability of attitude relies on the time-varying nature of the vector measurement to provide sufficient observability over time. Therefore, the applicability of the aforementioned estimation schemes are limited to the use of magnetometer measurements, since the Earth's magnetic field vector varies sufficiently over an orbit. An analytical investigation of observability of angular velocity alone for a torque-free spacecraft using a single inertially fixed vector measurement has been performed in [11]. It is shown that angular velocity is locally observable provided the spacecraft is not in an equilibrium spin condition with angular velocity parallel to the sun-vector. Previous authors have also developed angular velocity estimation algorithms from a single vector measurement [12–14], which would also be applicable in the inertially fixed vector measurement case.

In this paper, we treat the problem of online attitude estimation using sun-vector measurements only. Given the Earth's slow movement about the sun, sun-vector measurements can be treated as inertially fixed for practical purposes. We consider the case of a passively stabilized spacecraft utilizing permanent magnets and magnetic hysteresis rods. It was demonstrated with numerical examples based on real flight data in [6, 15] that it is indeed possible to estimate attitude and angular velocity for such spacecraft using only sun-vector measurements. In [15], a constrained batch optimization optimization problem is proposed to determine the entire history of attitude and angular velocity, as well as identifying the permanent magnet and hysteresis rod parameters. The purpose of this optimization procedure is primarily to estimate these magnetic parameters for calibration purposes. The determination of attitude and angular velocity in [15] is a by-product of the batch optimization needed to determine the magnetic parameters. This constrained batch optimization procedure is suitable for off-line implementation. The focus of the present paper is on attitude estimation schemes that are implementable in real-time. In [6], the hysteresis rods are treated as negligible disturbances, and a MEKF is formulated for real-time estimation of the attitude and angular velocity only. As is demonstrated with an example in this paper, it is possible to neglect the hysteresis rods in the scenario considered in [6], since the hysteresis rods are much smaller than the permanent magnets. When the hysteresis rods are more sizable, a different approach is needed and two such approaches are proposed in this paper. In addition, as demonstrated numerically in the present paper, neglecting the hysteresis rods (when applicable) comes with a penalty of reduced attitude estimation accuracy. Finally, neither [15] nor [6] present any analytical study of observability of the states and parameters to be estimated. By contrast, a significant portion of this paper is devoted to observability analyses.

In this paper, we first perform an analytical investigation of observability for spacecraft with known constant magnetic dipole (as is the scenario in the MEKF in [6]), demonstrating that under a reasonable assumption on the Earth's magnetic field, both attitude and angular velocity are indeed locally observable from a single inertially fixed vector measurement. It is then shown that if the magnetic dipole is only partially known, then the remaining unknown part of the magnetic dipole is observable also. Justified by these observability results, three state estimation schemes are presented

together with numerical examples. The first is a MEKF similar to that in [6] which neglects the hysteresis rods, and estimates attitude and angular velocity only. The second is a MEKF incorporating the hysteresis rod dipoles, but treats them as constant (they are nearly constant at steady-state). This MEKF estimates attitude, angular velocity and the hysteresis rod magnetic dipole moments. The third is a cubature Kalman filter (CKF) [16], which incorporates the discontinuous hysteresis rod dynamics. This CKF estimates attitude, angular velocity and the hysteresis rod magnetic flux densities. The state estimation schemes increase in computational complexity from the first to the third, and it is demonstrated with numerical examples that the steady-state state estimation performance also improves from the first to the third. The final two state estimation schemes are applicable for any passively magnetically stabilized spacecraft, while the first is applicable only if the hysteresis rods are significantly smaller than the permanent magnets.

II. Preliminaries

In this paper, the $n \times n$ identity matrix will be denoted by 1_n, and the $n \times m$ matrix of zeros will be denoted by $0_{n\times m}$. When the dimension is clear from context, the subscript will be omitted. The Euclidean norm of the vector $x \in \mathbb{R}^n$ is denoted by $\|x\|_2$.

Consider the system described by

$$\dot{x} = f(x,t), \tag{1}$$

with initial condition $x(t_0) = x_0$, where $x \in \mathbb{R}^{n_x}$ is the system state and $f(x,t) : \mathbb{R}^{n_x} \times \mathbb{R} \to \mathbb{R}^{n_x}$ is piecewise continuous in t, and locally Lipschitz continuous in x, uniformly in t. Under the Lipschitz condition, the solution of (1) exists on some interval $[t_0, t_0 + \delta]$ and is uniquely determined by the initial condition $x(t_0)$ [17]. Consider in addition, the measurement equation

$$y = h(x), \tag{2}$$

where $y \in \mathbb{R}^{n_y}$ is the measurement and $h(x) : \mathbb{R}^{n_x} \to \mathbb{R}^{n_y}$.

Definition 1. Consider two solutions $x_1(t)$ and $x_2(t)$ of (1). Then, $h(x)$ is said to distinguish $x_1(t)$ and $x_2(t)$ if $h(x_1(t)) \neq h(x_2(t))$ for some $t \in \mathbb{R}$.

Definition 2. We say that a solution $x(t)$ of (1) is locally distinguishable under $h(x)$ at time $\bar{t} \in \mathbb{R}$ if there exists a neighborhood $B(x(\bar{t}))$ of $x(\bar{t})$ such that $h(x)$ distinguishes $x(t)$ from every other solution of (1) passing through $B(x(\bar{t}))$ at time $\bar{t}$.

Theorem 1. [18] Let $A \subset \mathbb{R}^n$ and $B \subset \mathbb{R}^m$ be open sets, and $F : A \to B$ a C^∞ mapping. Suppose $[\partial F/\partial x]_x$ has rank k for all $x \in A$. For each point $x^o \in A$, there exist a neighborhood A_o of x^o in A and a neighborhood B_o of $F(x^o)$ in B, two open sets $U \subset \mathbb{R}^n$ and $V \subset \mathbb{R}^m$, and two diffeomorphisms $G : U \to A_o$ and $H : B_o \to V$ such that $H \circ F \circ G(U) \subset V$ and such that for all $(x_1, ..., x_n) \in U$, $(H \circ F \circ G)(x_1, ..., x_n) = (x_1, ..., x_k, 0, ..., 0)$.

Define the mapping $P_k : \mathbb{R}^n \to \mathbb{R}^m$ by $P_k(x_1, ..., x_n) = (x_1, ..., x_k, 0, ..., 0)$. Since H and G are invertible, it follows that $F = H^{-1} \circ P_k \circ G^{-1}$, which holds at all points of A_o.

Corollary 1. Consider a mapping F as in Theorem 1. Suppose that $[\partial F/\partial x]$ has rank n at a point $x_o \in A$. Then, there exists a neighborhood $A_o \subset A$ of x_o such that the mapping $F : A_o \to F(A_o)$ is one-to-one.

Proof. Since $[\partial F/\partial x]_{x_o}$ has rank n the minimum eigenvalue of $[\partial F/\partial x]_{x_o}[\partial F/\partial x]^T_{x_o}$ is positive. By continuity, there exists a neighborhood $C_o \subset A$ of x_o minimum eigenvalue of $[\partial F/\partial x]_x[\partial F/\partial x]^T_x$ is positive for all $x \in C_o$, which implies that $[\partial F/\partial x]_x$ has rank n for all $x \in C_o$. Theorem 1 may now be applied to obtain the neighborhood $A_o \subset C_o$ of x_o. The mapping P_n defined above is one-to-one. Consequently, the mapping F is the composition of one-to-one functions. □

Proposition 1. Consider two solutions $x_1(t)$ and $x_2(t)$ of equation (1), and define $y_1(t) = h(x_1(t))$ and $y_2(t) = h(x_2(t))$. Assume that $y_1(t)$ and $y_2(t)$ are n-times differentiable for some $n \geq 0$. Suppose that there exists a $t' \in \mathbb{R}$ such that $d^i y_1/dt^i(t') \neq d^i y_2/dt^i(t')$, for some $0 \leq i \leq n$. Then, $h(x)$ distinguishes $x_1(t)$ and $x_2(t)$.

Proof. Suppose to the contrary that there does exist a $t' \in \mathbb{R}$ such that $d^i y_1/dt^i(t') \neq d^i y_2/dt^i(t')$, for some $0 \leq i \leq n$, but that $h(x)$ does not distinguish $x_1(t)$ and $x_2(t)$. Then, $y_1(t) \equiv y_2(t)$, which implies that $d^i y_1/dt^i(t') \equiv d^i y_2/dt^i(t')$ for all $i = 0, ..., n$, which is a contradiction. □

III. Problem Formulation

This section examines the observability of a rigid-body spacecraft's attitude and angular velocity from a single inertially fixed vector measurement. The spacecraft body-frame is denoted $\mathcal{F}_b$, while the inertial frame is denoted $\mathcal{F}_I$. The spacecraft attitude is represented by the rotation matrix $C_{bI} \in SO(3)$ mapping coordinates of vectors from $\mathcal{F}_I$ to $\mathcal{F}_b$. Note that $SO(3) = \{C \in \mathbb{R}^{3\times 3} : C^TC = 1, \det C = 1\}$. The spacecraft inertial angular velocity is denoted ω_{bI}, and the spacecraft kinematics are given by Poisson's equations [19, pp. 22–23]

$$\dot{C}_{bI} = -\omega_{bI}^{\times} C_{bI}, \tag{3}$$

where for any vector $a, b \in \mathbb{R}^3$, $a^{\times} \in \mathbb{R}^3$ satisfies the cross-product relation $a^{\times}b = a \times b$. The dynamics of a rigid-body spacecraft with magnetic torque is given by [19, pp. 59, 264–265]

$$I\dot{\omega}_{bI} = -\omega_{bI}^{\times} I\omega_{bI} + m_b^{\times} C_{bI} b_I(t), \tag{4}$$

where $I \in \mathbb{R}^{3\times 3}$ is the spacecraft moment of inertia matrix about the spacecraft's center of mass, $m_b \in \mathbb{R}^3$ is the spacecraft magnetic dipole moment in body coordinates, and $b_I(t) \in \mathbb{R}^3$ is the local Earth magnetic field flux density vector in inertial coordinates. In addition, we consider a single vector measurement of the form

$$s_b = C_{bI} s_I \tag{5}$$

where $s_I \in \mathbb{R}^3$ is a constant non-zero vector.

It is assumed that m_b is bounded and continuous, and $b_I(t)$ is bounded and differentiable. Note that under these conditions, it follows that solutions of (3) and (4) are uniquely determined by the initial condition $(C_{bI}(t_0), \omega_{bI}(t_0))$. Furthermore, a simple argument will show that all solutions exist on $t \in \mathbb{R}$. First, $C_{bi}(t)$ lies in $SO(3)$, which is bounded. To this end, consider the rigid body's kinetic energy

$$T = \frac{1}{2}\omega_{bI}^T I \omega_{bI}. \tag{6}$$

From (6), we have

$$\lambda_{\min}(I)\|\omega_{bI}\| \leq 2T(\omega_{bI}) \leq \lambda_{\max}(I)\|\omega_{bI}\|^2, \tag{7}$$

where $\lambda_{\min}(I) > 0$ and $\lambda_{\max}(I) > 0$ denote the minimum and maximum eigenvalues of I, respectively. Now, consider the unique solution of (3) and (4) corresponding to initial condition $(C_{bI}(t_0), \omega_{bI}(t_0))$, for some $t_0 \in \mathbb{R}$. Along this solution, one obtains from (6) and (4) that

$$\dot{T} = \frac{\partial T}{\partial \omega_{bI}} \dot{\omega}_{bI} = \omega_{bI}^T m_b^\times C_{bI} b_I(t). \tag{8}$$

Since $m_b^\times C_{bI} b_I(t)$ is bounded, there exists a $\tau_d \in \mathbb{R}$ such that $\|m_b^\times C_{bI} b_I(t)\|_2 \leq \tau_d$ for all $t \in \mathbb{R}$. Consequently, application of Young's inequality to (8) gives

$$-\frac{\|\omega_{bI}\|^2}{2} - \frac{\tau_d^2}{2} \leq \dot{T}(t) \leq \frac{\|\omega_{bI}\|^2}{2} + \frac{\tau_d^2}{2}, \tag{9}$$

and application of (7) gives

$$-\frac{T}{\lambda_{\min}(I)} - \frac{\tau_d^2}{2} \leq \dot{T} \leq \frac{T}{\lambda_{\min}(I)} + \frac{\tau_d^2}{2}, \tag{10}$$

Application of the comparison principle [17] to (10) yields

$$T(t) \leq \begin{cases} e^{(t-t_0)/\lambda_{\min}(I)} \left[T(t_0) + \tau_d^2/(2\lambda_{\min}(I))\right] - \tau_d^2/(2\lambda_{\min}(I)), & t \geq t_0, \\ e^{(t_0-t)/\lambda_{\min}(I)} \left[T(t_0) + \tau_d^2/(2\lambda_{\min}(I))\right] - \tau_d^2/(2\lambda_{\min}(I)), & t \leq t_0, \end{cases} \tag{11}$$

The inequalities in (11) show that the kinetic energy $T(t)$ can have at most exponential growth either forwards or backwards in time, and finite for all $t \in \mathbb{R}$. Therefore, it must be that $(C_{bI}(t), \omega_{bI}(t))$ exists for all $t \in \mathbb{R}$.

A. Indistinguishability for a Torque-Free Spacecraft

For completeness, we shall first consider the distinguishability of equations (3) and (4) under measurement (5) in the torque-free case ($m_b = 0$). To this end, let $(C_{bI}(t), \omega_{bI}(t))$ be any solution of (3) and (4), together with measurement

$$s_b(t) = C_{bI}(t) s_I. \tag{12}$$

Note that equation (4) is *independent* of the attitude C_{bI}, so it can be solved independently. Next, consider another solution $(\bar{C}_{bI}(t), \bar{\omega}_{bI}(t))$ of (3) and (4), where

$$\bar{C}_{bI}(t) = C_{bI}(t) C_{\phi,sI}, \;\; \bar{\omega}_{bI}(t) = \omega_{bI}(t), \tag{13}$$

with corresponding measurement

$$\bar{s}_b(t) = \bar{C}_{bI}(t)s_I \tag{14}$$

where

$$C_{\phi,sI} = \cos\phi 1_3 + (1-\cos\phi)s_I s_I^T - \sin\phi s_I^\times, \tag{15}$$

for some fixed $\phi \in \mathbb{R}$. It is straightforward to show that $(\bar{C}_{bI}(t), \bar{\omega}_{bI}(t))$ is indeed a solution of (3) and (4). Note that $C_{\phi,sI}$ corresponds to a rotation about s_I through angle ϕ [19, pp. 10–12], and consequently $C_{\phi,sI}s_I = s_I$. Therefore, $\bar{s}_b(t) = s_b(t)$ for all $t \in \mathbb{R}$. Consequently, the solution $(C_{bI}(t), \omega_{bI}(t))$ is *indistinguishable* from $(\bar{C}_{bI}(t), \bar{\omega}_{bI}(t))$ under the measurement in (5). Furthermore, by making $\phi \in \mathbb{R}$ in (15) small enough, the solution $(\bar{C}_{bI}(t), \bar{\omega}_{bI}(t))$ can be made arbitrarily close to $(C_{bI}(t), \omega_{bI}(t))$ at any time $t \in \mathbb{R}$. Consequently, *no* solution $(C_{bI}(t), \omega_{bI}(t))$ of (3) and (4) is locally distinguishable *anywhere* under the single inertially fixed vector measurement in (3), as is well-known.

B. Local Distinguishability for a Spacecraft with Known Magnetic Torque

It is not surprising that attitude is not distinguishable with a single inertially fixed measurement vector for a torque-free spacecraft, as demonstrated in Section III A. The reason for this is that the equation governing the angular velocity (4) is decoupled from the equation governing the attitude when $m_b = 0$. One could expect that the distinguishability of solutions will improve if the spacecraft is affected by an attitude-dependent torque. One such torque is a magnetic torque, and this type of situation arises in spacecraft with passive magnetic stabilization.

In this section we consider the case where the magnetic dipole m_b is known and constant. To examine distinguishability, we shall make use of Proposition 1 and Corollary 1. Differentiating (5) twice, and making used of equations (3) and (4) gives the system of equations

$$s_b = C_{bI}s_I, \tag{16}$$

$$\dot{s}_b = -\omega_{bI}^\times C_{bI}s_I, \tag{17}$$

$$\ddot{s}_b = (C_{bI}s_I)^\times I^{-1}(m_b^\times C_{bI}b_I(t) - \omega_{bI}^\times I\omega_{bI}) + \omega_{bI}^\times\omega_{bI}^\times C_{bI}s_I. \tag{18}$$

Consider a solution $(\bar{C}_{bI}(t), \bar{\omega}_{bI}(t)) \in SO(3) \times \mathbb{R}^3$ of (3) and (4). By Proposition 1, this solution is locally distinguishable at time $t \in \mathbb{R}$, if equations (16), (17) and (18) are locally uniquely solvable at $t \in \mathbb{R}$. Since the configuration manifold of the solution is $SO(3) \times \mathbb{R}^3$, we need to examine the local solvability in a local coordinate chart centered on the solution $(\bar{C}_{bI}(t), \bar{\omega}_{bI}(t))$. Such a coordinate chart can readily be constructed by considering the Lie Algebra $so(3)$ associated with $SO(3)$. In particular, we can locally represent C_{bI} around $\bar{C}_{bI}(t)$ by defining

$$C_{bI}(p,t) = \exp(-p^\times)\bar{C}_{bI}(t), \tag{19}$$

where $p \in \mathbb{R}^3$, and $\exp(\cdot)$ denotes the matrix exponential. Similarly, we define

$$\omega_{bI}(q,t) = \bar{\omega}_{bI}(t) + q, \tag{20}$$

where $q \in \mathbb{R}^3$. Noting that $(C_{bI}(0,t), \omega_{bI}(0,t)) = (\bar{C}_{bI}(t), \bar{\omega}_{bI}(t))$, the pair $(p,q) \in \mathbb{R}^3 \times \mathbb{R}^3$ defines a local coordinate chart of $SO(3) \times \mathbb{R}^3$ centered on the solution $(\bar{C}_{bI}(t), \bar{\omega}_{bI}(t))$. By Corollary 1, to determine local distinguishability of $(\bar{C}_{bI}(t), \bar{\omega}_{bI}(t))$, we examine the rank of the Jacobian of equations (16), (17) and (18) with respect to (p,q) about the solution $(\bar{C}_{bI}(t), \bar{\omega}_{bI}(t))$. Noting that for any $a \in \mathbb{R}^3$,

$$\left.\frac{\partial (C_{bI}(p,t)a)}{\partial p}\right|_{p=0} = (\bar{C}_{bI}(t)a)^\times,$$

the Jacobian of the system of equations (16), (17) and (18) with respect to (p,q) is obtained as

$$J_{p,q}(t) \triangleq \begin{bmatrix} \left.\frac{\partial s_b}{\partial p}\right|_{0,0} & \left.\frac{\partial s_b}{\partial q}\right|_{0,0} \\ \left.\frac{\partial \dot{s}_b}{\partial p}\right|_{0,0} & \left.\frac{\partial \dot{s}_b}{\partial q}\right|_{0,0} \\ \left.\frac{\partial \ddot{s}_b}{\partial p}\right|_{0,0} & \left.\frac{\partial \ddot{s}_b}{\partial q}\right|_{0,0} \end{bmatrix} = \begin{bmatrix} \bar{s}_b(t)^\times & 0 \\ -\bar{\omega}_{bI}(t)^\times \bar{s}_b(t)^\times & \bar{s}_b(t)^\times \\ A(t) & B(t) \end{bmatrix} \tag{21}$$

where

$$\begin{aligned} A(t) &= \left[I^{-1}(\bar{\omega}_{bI}(t)^\times I \bar{\omega}_{bI}(t) - m_b^\times \bar{b}_b(t))\right]^\times \bar{s}_b(t)^\times + \bar{s}_b(t)^\times I^{-1} m_b^\times \bar{b}_b(t)^\times \\ &\quad + \bar{\omega}_{bI}(t)^\times \bar{\omega}_{bI}(t)^\times \bar{s}_b(t)^\times, \end{aligned} \tag{22}$$

$$B(t) = \bar{s}_b(t)^\times I^{-1}\left((I\bar{\omega}_{bI}(t))^\times - \bar{\omega}_{bI}(t)^\times I\right) - \bar{\omega}_{bI}(t)^\times \bar{s}_b(t)^\times - (\bar{\omega}_{bI}(t)^\times \bar{s}_b(t))^\times, \tag{23}$$

and $\bar{s}_b(t)$ is given in (14) and

$$\bar{b}_b(t) = \bar{C}_{bI}(t) b_I(t), \tag{24}$$

is the Earth magnetic field vector in the spacecraft body frame along the solution $\bar{C}_{bI}(t)$, respectively.

We now examine the null-space of the Jacobian $J_{p,q}(t)$. To this end, let $a, b \in \mathbb{R}^3$, and suppose that

$$J_{p,q}(t) \begin{bmatrix} a^T & b^T \end{bmatrix}^T = 0. \tag{25}$$

Then, from the first two rows in (21), we find that we must have $a = \lambda_1 \bar{s}_b(t)$ and $b = \lambda_2 \bar{s}_b(t)$, for some $\lambda_1, \lambda_2 \in \mathbb{R}$. Furthermore, since $\bar{s}_b(t) \neq 0$, the Jacobian $J_{p,q}$ has a non-trivial null-space if and only if either $\lambda_1 \neq 0$ or $\lambda_2 \neq 0$ (or both). From (22) and (23), we now have

$$A(t)a = \lambda_1 \bar{s}_b(t)^\times I^{-1} m_b^\times \bar{b}_b(t)^\times \bar{s}_b(t), \tag{26}$$

$$B(t)b = \lambda_2 \bar{s}_b(t)^\times I^{-1} \bar{\omega}_{bI}(t)^\times D \bar{s}_b(t), \tag{27}$$

where $D = \text{trace}[I] - 2I$, and the following identity (which can be verified by direct expansion) has been used

$$I\bar{\omega}_{bI}(t))^\times - \bar{\omega}_{bI}(t)^\times I + I\bar{\omega}_{bI}(t) = \bar{\omega}_{bI}(t)^\times D.$$

Note that D is positive-definite. To see why, decompose $I = E\,\text{diag}[I_1, I_2, I_3]E^T$, where I_1, I_2, I_3 are the principal inertias and $E \in SO(3)$ [20]. Then, $D = E\,\text{diag}[a, b, c]E^T$, where $a = I_2 - I_1 + I_3 > 0$, $b = I_3 - I_2 + I_1 > 0$, and $c = I_1 - I_3 + I_2 > 0$ [19, p. 86].

Consequently, for (25) to hold, the third row in (21) leads to the necessary and sufficient condition

$$\bar{s}_b(t)^\times I^{-1} \left(\lambda_1 m_b^\times \bar{b}_b(t)^\times + \lambda_2 \bar{\omega}_{bI}(t)^\times D\right) \bar{s}_b(t) = 0. \tag{28}$$

This in turn holds if and only if

$$\left(\lambda_1 m_b^\times \bar{b}_b(t)^\times + \lambda_2 \bar{\omega}_{bI}(t)^\times D\right) \bar{s}_b(t) = -\lambda_3 I \bar{s}_b(t), \tag{29}$$

for some $\lambda_3 \in \mathbb{R}^3$, which can be written as

$$K\lambda = 0, \tag{30}$$

where $\lambda = [\lambda_1 \ \lambda_2 \ \lambda_3]^T$ and

$$K = \begin{bmatrix} m_b^\times \bar{b}_b(t)^\times \bar{s}_b(t) & \bar{\omega}_{bI}(t)^\times D \bar{s}_b(t) & I\bar{s}_b(t) \end{bmatrix}. \tag{31}$$

It can be seen from (31) that $\lambda = [0\ 0\ \lambda_3]^T$ is not a solution of (30) (since $\bar{s}_b(t) \neq 0$). Therefore, it follows that the Jacobian $J_{p,q}(t)$ has full column rank if and only if $\det K \neq 0$, that is

$$(I\bar{s}_b(t))^T \left(m_b^\times \bar{b}_b(t)^\times \bar{s}_b(t)\right)^\times \left(\bar{\omega}_{bI}(t)^\times D\bar{s}_b(t)\right) \neq 0. \tag{32}$$

The condition in (32) has a simple geometric interpretation. Namely, $J_{p,q}(t)$ has full column rank if and only if the following conditions hold.

1. $\bar{\omega}_{bI}(t)^\times D\bar{s}_b(t) \neq 0$
2. $m_b^\times \bar{b}_b(t)^\times \bar{s}_b(t) \neq 0$
3. $m_b^\times \bar{b}_b(t)^\times \bar{s}_b(t)$ is not parallel to $\bar{\omega}_{bI}(t)^\times D\bar{s}_b(t)$
4. $I\bar{s}_b(t) \notin \text{span}\{m_b^\times \bar{b}_b(t)^\times \bar{s}_b(t), \bar{\omega}_{bI}(t)^\times D\bar{s}_b(t)\}$

Associated with (32), define the time-varying set

$$\mathcal{F}(t) = \{(C,\omega) \in SO(3)\times\mathbb{R}^3 : (ICs_I)^T \left(m_b^\times (Cb_I(t))^\times Cs_I\right)^\times \left(\omega(t)^\times DCs_I\right) = 0\}. \tag{33}$$

For fixed $t \in \mathbb{R}$, the set $\mathcal{F}(t)$ is a hypersurface in $SO(3)\times\mathbb{R}^3$. Given the significant variability of the Earth's magnetic field throughout an orbit [21], it is very reasonable to make the following assumption:

Assumption 1 For any solution $(C_{bI}(t), \omega_{bI}(t)) \in SO(3)\times\mathbb{R}^3$ of (3) and (4) with constant m_b, the set of times $\mathcal{T} = \{t \in \mathbb{R} : (C_{bI}(t), \omega_{bI}(t)) \in \mathcal{F}(t)\}$ has measure zero.

We now obtain the following theorem.

Theorem 2. Under Assumption 1, every solution $(C_{bI}(t), \omega_{bI}(t)) \in SO(3)\times\mathbb{R}^3$ of (3) and (4) is locally distinguishable under the measurement $s_b = C_{bI}s_I$ for almost all $t \in \mathbb{R}$.

Proof. Consider a solution $(\bar{C}_{bI}(t), \bar{\omega}_{bI}(t)) \in SO(3)\times\mathbb{R}^3$ of (3) and (4), with corresponding mea-

surement $\bar{s}_b(t) = \bar{C}_{bI}(t)s_I$. Corresponding to equations (16), (17) and (18), define the function

$$F(x,t) = \begin{bmatrix} C_{bI}(p,t)s_I \\ -\omega_{bI}(q,t)^\times C_{bI}(p,t)s_I \\ (C_{bI}(p,t)s_I)^\times I^{-1}(m_b^\times C_{bI}(p,t)b_I(t) - \omega_{bI}(q,t)^\times I\omega_{bI}(q,t)) + \omega_{bI}(q,t)^\times\omega_{bI}(q,t)^\times C_{bI}(p,t)s_I \end{bmatrix}, \tag{34}$$

where $x = (p,q)$, and $C_{bI}(q,t)$ and $\omega_{bI}(q,t)$ are defined in (19) and (20). Thus, we have $\begin{bmatrix} \bar{s}_b(t) & \dot{\bar{s}}_b(t) & \ddot{\bar{s}}_b(t) \end{bmatrix}^T = F(0,t)$.

By Assumption 1, the Jacobian $\partial F/\partial x$ evaluated along $(\bar{C}_{bI}(t), \bar{\omega}_{bI}(t))$ has full column rank for almost all $t \in \mathbb{R}$. By Corollary 1, for each $t \notin \mathcal{T}$ there exists a neighborhood $A(t)$ of $x = 0$ such that the mapping $F(x,t) : A(t) \to F(A(t))$ in (34) is one-to-one. Consider any other solution $(C'_{bI}(t), \omega'_{bI}(t))$ of (3) and (4) passing through $A(t)$ at time t, in the sense that $(C'_{bI}(t), \omega'_{bI}(t)) = (C_{bI}(p',t), \omega_{bI}(q',t))$ for some $x' = (p',q') \in A(t)$ with $x' \neq 0$, together with corresponding measurement $s'_b(t) = C'_{bI}(t)s_I$. By (16), (17), (18) and (34), we have $\begin{bmatrix} s'_b(t) & \dot{s}'_b(t) & \ddot{s}'_b(t) \end{bmatrix}^T = F(x',t)$. Since $F(x,t)$ is one-to-one on $A(t)$, $F(0,t) \neq F(x',t)$, which implies that it is impossible to have $s'_b(t) = \bar{s}_b(t)$, $\dot{s}'_b(t) = \dot{\bar{s}}_b(t)$ and $\ddot{s}'_b(t) = \ddot{\bar{s}}_b(t)$ simultaneously. Consequently, by Proposition 1, it follows that $s_b = C_{bI}s_I$ distinguishes $(\bar{C}_{bI}(t), \bar{\omega}_{bI}(t))$ and $(C'_{bI}(t), \omega'_{bI}(t))$. □

C. Local Distinguishability for a Spacecraft with Partially Known Magnetic Torque

In this section, we examine the local distinguishability in the case where the

$$m_b = m_p e_2 + m_{h1}e_1 + m_{h3}e_3, \tag{35}$$

where $e_i \in \mathbb{R}^3$ for $i = 1,2,3$ constitute the standard basis for $\mathbb{R}^3$, m_p is a known constant dipole moment (aligned with the spacecraft y-axis), and m_{h1} and m_{h3} are constant unknown dipole moments. It is desired to be estimate C_{bI}, ω_{bI} and m_{h1}, m_{h3}. The motivation for this problem can be found in Section IV, where a permanent magnet with known dipole moment is aligned with the spacecraft body y-axis, and a pair of magnetic hysteresis rods are aligned with the spacecraft x- and z-axes respectively. The hysteresis rod dipole moments are time-varying and unknown, but as

shown in Section IV, they do tend towards nearly constant steady-state values. Defining

$$m_h = \begin{bmatrix} m_{h1} & m_{h3} \end{bmatrix}^T, \tag{36}$$

we set

$$m_b = m_p e_2 + \begin{bmatrix} e_1 & e_3 \end{bmatrix} m_h. \tag{37}$$

in equations (3) and (4), and append the equation

$$\dot{m}_h = 0. \tag{38}$$

We now consider the local distinguishability of solutions of (3), (4) and (38) with (37) again under the single inertially fixed vector measurement given by (5). We proceed as in Section III B. Writing $\ddot{s}_b$ in (18) as

$$\ddot{s}_b = s_b^\times \dot{\omega}_{bI} + \omega_{bI}^\times \omega_{bI}^\times s_b, \tag{39}$$

differentiating one further time and making use of (17) and the identities $(a^\times)^3 = -(a^T a)a^\times$ and $(a^\times b)^\times = a^\times b^\times - b^\times a^\times$ for any $a, b \in \mathbb{R}^3$, leads to

$$\dddot{s}_b = s_b^\times \ddot{\omega}_{bI} - (3\omega_{bI}^\times s_b^\times - 2 s_b^\times \omega_{bI}^\times)\dot{\omega}_{bI} + (\omega_{bI}^T \omega_{bI})\omega_{bI}^\times s_b, \tag{40}$$

where $\dot{\omega}_{bI}$ is given in (4), and using (4) and (38)

$$\ddot{\omega}_{bI} = I^{-1}\left((m_p e_2)^\times \dot{b}_b + ([e_1\ e_3]m_h)^\times \dot{b}_b + [(I\omega_{bI})^\times - \omega_{bI}^\times I]\dot{\omega}_{bI}\right), \tag{41}$$

with

$$\dot{b}_b = -\omega_{bI}^\times b_b + \frac{\partial b_b}{\partial t},\ \ \frac{\partial \dot{b}_b}{\partial t} = C_{bI}\dot{b}_I. \tag{42}$$

We now proceed as in Section III B. Consider a solution $(\bar{C}_{bI}(t), \bar{\omega}_{bI}(t), \bar{m}_h(t)) \in SO(3) \times \mathbb{R}^3 \times \mathbb{R}^2$ of (3), (4) and (38) with (37), with corresponding measurement given by (14). Similar to Section III B, we define a local coordinate chart $(p, q, r) \in \mathbb{R}^3 \times \mathbb{R}^3 \times \mathbb{R}^2$ of the configuration manifold $SO(3) \times \mathbb{R}^3 \times \mathbb{R}^2$, centered on $(\bar{C}_{bI}(t), \bar{\omega}_{bI}(t), \bar{m}_h(t))$, by (19), (20) and

$$m_h(r) = \bar{m}_h + r. \tag{43}$$

Note that $(C_{bI}(0,t), \omega_{bI}(0,t), m_h(0)) = (\bar{C}_{bI}(t), \bar{\omega}_{bI}(t), \bar{m}_h(t))$. Then, the Jacobian of the system of equations given by (16), (17), (39) and (40) with respect to (p,q,r) is given by

$$J_{p,q,r}(t) \triangleq \begin{bmatrix} \frac{\partial s_b}{\partial p}\Big|_{0,0,0} & \frac{\partial s_b}{\partial q}\Big|_{0,0,0} & \frac{\partial s_b}{\partial r}\Big|_{0,0,0} \\ \frac{\partial \dot{s}_b}{\partial p}\Big|_{0,0,0} & \frac{\partial \dot{s}_b}{\partial q}\Big|_{0,0,0} & \frac{\partial \dot{s}_b}{\partial r}\Big|_{0,0,0} \\ \frac{\partial \ddot{s}_b}{\partial p}\Big|_{0,0,0} & \frac{\partial \ddot{s}_b}{\partial q}\Big|_{0,0,0} & \frac{\partial \ddot{s}_b}{\partial r}\Big|_{0,0,0} \\ \frac{\partial \dddot{s}_b}{\partial p}\Big|_{0,0,0} & \frac{\partial \dddot{s}_b}{\partial q}\Big|_{0,0,0} & \frac{\partial \dddot{s}_b}{\partial r}\Big|_{0,0,0} \end{bmatrix} = \begin{bmatrix} \bar{s}_b(t)^\times & 0 & 0 \\ -\bar{\omega}_{bI}(t)^\times \bar{s}_b(t)^\times & \bar{s}_b(t)^\times & 0 \\ \frac{\partial \ddot{s}_b}{\partial p}\Big|_{0,0,0} & \frac{\partial \ddot{s}_b}{\partial q}\Big|_{0,0,0} & \frac{\partial \ddot{s}_b}{\partial r}\Big|_{0,0,0} \\ \frac{\partial \dddot{s}_b}{\partial p}\Big|_{0,0,0} & \frac{\partial \dddot{s}_b}{\partial q}\Big|_{0,0,0} & \frac{\partial \dddot{s}_b}{\partial r}\Big|_{0,0,0} \end{bmatrix}, \quad (44)$$

where (dropping the time argument for brevity)

$$\begin{aligned}
\frac{\partial \ddot{s}_b}{\partial p}\Big|_{0,0,0} &= -\dot{\bar{\omega}}_{bI}^\times \bar{s}_b^\times + \bar{s}_b^\times \frac{\partial \dot{\omega}_{bI}}{\partial p}\Big|_{0,0,0} + \bar{\omega}_{bI}^\times \bar{\omega}_{bI}^\times \bar{s}_b^\times, \\
\frac{\partial \ddot{s}_b}{\partial q}\Big|_{0,0,0} &= \bar{s}_b^\times \left(\frac{\partial \dot{\omega}_{bI}}{\partial q}\Big|_{0,0,0} + \bar{\omega}_{bI}^\times \right) - 2\bar{\omega}_{bI}^\times \bar{s}_b^\times, \\
\frac{\partial \ddot{s}_b}{\partial r}\Big|_{0,0,0} &= \bar{s}_b^\times \frac{\partial \dot{\omega}_{bI}}{\partial r}\Big|_{0,0,0}, \\
\frac{\partial \dddot{s}_b}{\partial p}\Big|_{0,0,0} &= \bar{s}_b^\times \frac{\partial \ddot{\omega}_{bI}}{\partial p}\Big|_{0,0,0} + \left(-\ddot{\bar{\omega}}_{bI}^\times + 3\bar{\omega}_{bI}^\times \dot{\bar{\omega}}_{bI}^\times - 2\left(\bar{\omega}_{bI}^\times \dot{\bar{\omega}}_{bI}\right)^\times + (\bar{\omega}_{bI}^T \bar{\omega}_{bI})\bar{\omega}_{bI}^\times \right) \bar{s}_b^\times \\
&\quad - \left(3\bar{\omega}_{bI}^\times \bar{s}_b^\times - 2\bar{s}_b^\times \bar{\omega}_{bI}^\times \right) \frac{\partial \dot{\omega}_{bI}}{\partial p}\Big|_{0,0,0}, \\
\frac{\partial \dddot{s}_b}{\partial q}\Big|_{0,0,0} &= \bar{s}_b^\times \frac{\partial \ddot{\omega}_{bI}}{\partial q}\Big|_{0,0,0} + 3\left(\bar{s}_b^\times \dot{\bar{\omega}}_{bI}\right)^\times - 2\bar{s}_b^\times \dot{\bar{\omega}}_{bI}^\times - (\bar{\omega}_{bI}^T \bar{\omega}_{bI})\bar{s}_b^\times + 2\bar{\omega}_{bI}^\times \bar{s}_b \bar{\omega}_{bI}^T \\
&\quad - \left(3\bar{\omega}_{bI}^\times \bar{s}_b^\times - 2\bar{s}_b^\times \bar{\omega}_{bI}^\times \right) \frac{\partial \dot{\omega}_{bI}}{\partial q}\Big|_{0,0,0}, \\
\frac{\partial \dddot{s}_b}{\partial r}\Big|_{0,0,0} &= \bar{s}_b^\times \frac{\partial \ddot{\omega}_{bI}}{\partial r}\Big|_{0,0,0} - \left(3\bar{\omega}_{bI}^\times \bar{s}_b^\times - 2\bar{s}_b^\times \bar{\omega}_{bI}^\times \right) \frac{\partial \dot{\omega}_{bI}}{\partial r}\Big|_{0,0,0},
\end{aligned}$$

$$\dot{\bar{\omega}}_{bI} = I^{-1}\left(\bar{m}_b^\times \bar{b}_b - \bar{\omega}_{bI}^\times I \bar{\omega}_{bI} \right), \quad \bar{m}_b = m_p e_2 + \begin{bmatrix} e_1 & e_3 \end{bmatrix} \bar{m}_h, \quad \frac{\partial \dot{\omega}_{bI}}{\partial p}\Big|_{0,0,0} = I^{-1} \bar{m}_b^\times \bar{b}_b^\times,$$

$$\frac{\partial \dot{\omega}_{bI}}{\partial q}\Big|_{0,0,0} = I^{-1}\left((I\bar{\omega}_{bI})^\times - \bar{\omega}_{bI}^\times I \right), \quad \frac{\partial \dot{\omega}_{bI}}{\partial r}\Big|_{0,0,0} = -I^{-1} \bar{b}_b^\times \begin{bmatrix} e_1 & e_3 \end{bmatrix},$$

$$\ddot{\bar{\omega}}_{bI} = I^{-1}\left(\bar{m}_b^\times \dot{\bar{b}}_b + [(I\bar{\omega}_{bI})^\times - \bar{\omega}_{bI}^\times I]\dot{\bar{\omega}}_{bI} \right), \quad \dot{\bar{b}}_b = -\bar{\omega}_{bI}^\times \bar{b}_b + \frac{\partial \bar{b}_b}{\partial t}, \quad \frac{\partial \bar{b}_b}{\partial t} = \bar{C}_{bI} \dot{b}_I,$$

$$\frac{\partial \ddot{\omega}_{bI}}{\partial p}\Big|_{0,0,0} = I^{-1}\left(\bar{m}_b^\times \left(-\bar{\omega}_{bI}^\times \bar{b}_b^\times + \left(\frac{\partial \bar{b}_b}{\partial t} \right)^\times \right) + [(I\bar{\omega}_{bI})^\times - \bar{\omega}_{bI}^\times I] \frac{\partial \dot{\omega}_{bI}}{\partial p}\Big|_{0,0,0} \right),$$

$$\frac{\partial \ddot{\omega}_{bI}}{\partial q}\Big|_{0,0,0} = I^{-1}\left(\bar{m}_b^\times \bar{b}_b^\times + [(I\bar{\omega}_{bI})^\times - \bar{\omega}_{bI}^\times I] \frac{\partial \dot{\omega}_{bI}}{\partial q}\Big|_{0,0,0} + (I\dot{\bar{\omega}}_{bI})^\times - \dot{\bar{\omega}}_{bI}^\times I \right),$$

$$\left.\frac{\partial \ddot{\omega}_{bI}}{\partial r}\right|_{0,0,0} = I^{-1}\left(-\dot{\bar{b}}_b^{\times}\begin{bmatrix} e_1 & e_3 \end{bmatrix} + [(I\bar{\omega}_{bI})^{\times} - \bar{\omega}_{bI}^{\times} I]\left.\frac{\partial \dot{\omega}_{bI}}{\partial r}\right|_{0,0,0}\right).$$

Using the above expressions, and applying suitable row reductions to $J_{p,q,r}(t)$ in (44), one finds that $J_{p,q,r}(t)$ shares the same null-space as

$$\bar{J}_{p,q,r}(t) = \begin{bmatrix} \bar{s}_b(t)^{\times} & 0 & 0 \\ 0 & \bar{s}_b(t)^{\times} & 0 \\ \bar{A}(t) & \bar{B}(t) & \bar{D}(t) \\ \bar{E}(t) & \bar{F}(t) & \bar{G}(t) \end{bmatrix}, \tag{45}$$

where

$$\bar{A}(t) = \bar{s}_b(t)^{\times}\left.\frac{\partial \dot{\omega}_{bI}}{\partial p}\right|_{0,0,0},\ \ \bar{B}(t) = \bar{s}_b(t)^{\times}\left(\left.\frac{\partial \dot{\omega}_{bI}}{\partial q}\right|_{0,0,0} + \bar{\omega}_{bI}(t)^{\times}\right),\ \ \bar{D}(t) = \bar{s}_b(t)^{\times}\left.\frac{\partial \dot{\omega}_{bI}}{\partial r}\right|_{0,0,0},$$

$$\bar{E}(t) = \bar{s}_b(t)^{\times}\left(\left.\frac{\partial \ddot{\omega}_{bI}}{\partial p}\right|_{0,0,0} + 2\bar{s}_b(t)^{\times}\bar{\omega}_{bI}(t)^{\times}\left.\frac{\partial \dot{\omega}_{bI}}{\partial p}\right|_{0,0,0}\right),$$

$$\begin{aligned}\bar{F}(t) \ = \ & \bar{s}_b(t)^{\times}\left(\left.\frac{\partial \ddot{\omega}_{bI}}{\partial q}\right|_{0,0,0} + 2\bar{s}_b(t)^{\times}\bar{\omega}_{bI}(t)^{\times}\left.\frac{\partial \dot{\omega}_{bI}}{\partial q}\right|_{0,0,0} - 2\dot{\bar{\omega}}_{bI}^{\times} - 2\bar{\omega}_{bI}(t)\bar{\omega}_{bI}(t)^T\right) \\ & -3\bar{\omega}_{bI}(t)^{\times}(\bar{\omega}_{bI}(t)^T\bar{s}_b(t)) + 3\left(\bar{s}_b(t)^{\times}\dot{\bar{\omega}}_{bI}\right)^{\times},\end{aligned}$$

$$\bar{G}(t) = \bar{s}_b(t)^{\times}\left(\left.\frac{\partial \ddot{\omega}_{bI}}{\partial r}\right|_{0,0,0} + 2\bar{s}_b(t)^{\times}\bar{\omega}_{bI}(t)^{\times}\left.\frac{\partial \dot{\omega}_{bI}}{\partial r}\right|_{0,0,0}\right).$$

As in Section III B, we now identify the null-space of $\bar{J}_{p,q,r}(t)$. To this end, let $(a, b, c) \in \mathbb{R}^3 \times \mathbb{R}^3 \times \mathbb{R}^2$ satisfy

$$\bar{J}_{p,q,r}(t)\begin{bmatrix} a^T & b^T & c^T \end{bmatrix}^T = 0. \tag{46}$$

From (45), it follows that $a = \lambda_1 \bar{s}_b(t)$ and $b = \lambda_2 \bar{s}_b(t)$ for some $\lambda_1, \lambda_2 \in \mathbb{R}$. Substituting this into the third and fourth rows of (46) and using (45), leads to

$$\bar{s}_b(t)^{\times}\left(\lambda_1\left.\frac{\partial \dot{\omega}_{bI}}{\partial p}\right|_{0,0,0}\bar{s}_b(t) + \lambda_2\left(\left.\frac{\partial \dot{\omega}_{bI}}{\partial q}\right|_{0,0,0} + \bar{\omega}_{bI}(t)^{\times}\right)\bar{s}_b(t) + \left.\frac{\partial \dot{\omega}_{bI}}{\partial r}\right|_{0,0,0} c\right) = 0, \tag{47}$$

and

$$\begin{aligned} & \lambda_1 \bar{s}_b(t)^{\times}\left(\left.\frac{\partial \ddot{\omega}_{bI}}{\partial p}\right|_{0,0,0} + 2\bar{s}_b(t)^{\times}\bar{\omega}_{bI}(t)^{\times}\left.\frac{\partial \dot{\omega}_{bI}}{\partial p}\right|_{0,0,0}\right)\bar{s}_b(t) \\ & +\lambda_2 \bar{s}_b(t)^{\times}\left(\left.\frac{\partial \ddot{\omega}_{bI}}{\partial q}\right|_{0,0,0} + 2\bar{s}_b(t)^{\times}\bar{\omega}_{bI}(t)^{\times}\left.\frac{\partial \dot{\omega}_{bI}}{\partial q}\right|_{0,0,0} + \dot{\bar{\omega}}_{bI}^{\times} + \bar{\omega}_{bI}(t)\bar{\omega}_{bI}(t)^T\right)\bar{s}_b(t) \\ & +\bar{s}_b(t)^{\times}\left(\left.\frac{\partial \ddot{\omega}_{bI}}{\partial r}\right|_{0,0,0} + 2\bar{s}_b(t)^{\times}\bar{\omega}_{bI}(t)^{\times}\left.\frac{\partial \dot{\omega}_{bI}}{\partial r}\right|_{0,0,0}\right)c \ = \ 0, \end{aligned} \tag{48}$$

respectively. These in turn hold if and only if

$$\lambda_1 \left.\frac{\partial \dot{\omega}_{bI}}{\partial p}\right|_{0,0,0} \bar{s}_b(t) + \lambda_2 \left(\left.\frac{\partial \dot{\omega}_{bI}}{\partial q}\right|_{0,0,0} + \bar{\omega}_{bI}(t)^{\times} \right) \bar{s}_b(t) + \left.\frac{\partial \dot{\omega}_{bI}}{\partial r}\right|_{0,0,0} c = -\lambda_3 \bar{s}_b(t), \tag{49}$$

and

$$\begin{aligned} &\lambda_1 \left(\left.\frac{\partial \ddot{\omega}_{bI}}{\partial p}\right|_{0,0,0} + 2\bar{s}_b(t)^{\times} \bar{\omega}_{bI}(t)^{\times} \left.\frac{\partial \dot{\omega}_{bI}}{\partial p}\right|_{0,0,0} \right) \bar{s}_b(t) \\ +\lambda_2 &\left(\left.\frac{\partial \ddot{\omega}_{bI}}{\partial q}\right|_{0,0,0} + 2\bar{s}_b(t)^{\times} \bar{\omega}_{bI}(t)^{\times} \left.\frac{\partial \dot{\omega}_{bI}}{\partial q}\right|_{0,0,0} + \dot{\bar{\omega}}_{bI}^{\times} + \bar{\omega}_{bI}(t) \bar{\omega}_{bI}(t)^T \right) \bar{s}_b(t) \\ &+ \left(\left.\frac{\partial \ddot{\omega}_{bI}}{\partial r}\right|_{0,0,0} + 2\bar{s}_b(t)^{\times} \bar{\omega}_{bI}(t)^{\times} \left.\frac{\partial \dot{\omega}_{bI}}{\partial r}\right|_{0,0,0} \right) c \;=\; -\lambda_4 \bar{s}_b(t), \end{aligned} \tag{50}$$

for some $\lambda_3, \lambda_4 \in \mathbb{R}$. Equations (49) and (50) can be written in matrix form as

$$\bar{K}(\bar{C}_{bI}(t), \bar{\omega}_{bI}(t), \bar{m}_h(t)) \bar{\lambda} = 0, \tag{51}$$

where $\bar{\lambda}^T = \begin{bmatrix} \lambda_1 & \lambda_2 & \lambda_3 & \lambda_4 & c^T \end{bmatrix}$ and

$$\bar{K}(\bar{C}_{bI}, \bar{\omega}_{bI}, \bar{m}_h) = \begin{bmatrix} \bar{L}(\bar{C}_{bI}, \bar{\omega}_{bI}, \bar{m}_h) & \bar{M}(\bar{C}_{bI}, \bar{\omega}_{bI}, \bar{m}_h) \\ \bar{N}(\bar{C}_{bI}, \bar{\omega}_{bI}, \bar{m}_h) & \bar{O}(\bar{C}_{bI}, \bar{\omega}_{bI}, \bar{m}_h) \end{bmatrix}, \tag{52}$$

with

$$\bar{L}(\bar{C}_{bI}, \bar{\omega}_{bI}, \bar{m}_h) = \begin{bmatrix} \left.\frac{\partial \dot{\omega}_{bI}}{\partial p}\right|_{0,0,0} \bar{s}_b & \left(\left.\frac{\partial \dot{\omega}_{bI}}{\partial q}\right|_{0,0,0} + \bar{\omega}_{bI}^{\times} \right) \bar{s}_b & \bar{s}_b \end{bmatrix},$$

$$\bar{M}(\bar{C}_{bI}, \bar{\omega}_{bI}, \bar{m}_h) = \begin{bmatrix} 0_{3\times 1} & \left.\frac{\partial \dot{\omega}_{bI}}{\partial r}\right|_{0,0,0} \end{bmatrix},$$

$$\bar{N}(\bar{C}_{bI}, \bar{\omega}_{bI}, \bar{m}_h) =$$
$$\begin{bmatrix} \left(\left.\frac{\partial \ddot{\omega}_{bI}}{\partial p}\right|_{0,0,0} + 2\bar{s}_b^{\times} \bar{\omega}_{bI}^{\times} \left.\frac{\partial \dot{\omega}_{bI}}{\partial p}\right|_{0,0,0} \right) \bar{s}_b & \left(\left.\frac{\partial \ddot{\omega}_{bI}}{\partial q}\right|_{0,0,0} + 2\bar{s}_b^{\times} \bar{\omega}_{bI}^{\times} \left.\frac{\partial \dot{\omega}_{bI}}{\partial q}\right|_{0,0,0} + \dot{\bar{\omega}}_{bI}^{\times} + \bar{\omega}_{bI} \bar{\omega}_{bI}^T \right) \bar{s}_b & 0_{3\times 1} \end{bmatrix},$$

$$\bar{O}(\bar{C}_{bI}, \bar{\omega}_{bI}, \bar{m}_h) = \begin{bmatrix} \bar{s}_b(t) & \left(\left.\frac{\partial \ddot{\omega}_{bI}}{\partial r}\right|_{0,0,0} + 2\bar{s}_b^{\times} \bar{\omega}_{bI}^{\times} \left.\frac{\partial \dot{\omega}_{bI}}{\partial r}\right|_{0,0,0} \right) \end{bmatrix}.$$

Clearly, any non-trivial solution of (51) cannot simultaneously have $\lambda_1 = \lambda_2 = 0$ and $c = 0$. Therefore, $\bar{J}_{p,q,r}(t)$ and consequently $J_{p,q,r}(t)$ has full column rank if and only if $\det \bar{K}(\bar{C}_{bI}(t), \bar{\omega}_{bI}(t), \bar{m}_h(t)) \neq 0$. Unlike the case in Section III B, this does not have a nice geometric interpretation. However, as in Section III B, we can define the time-varying set

$$\bar{\mathcal{F}}(t) = \{(C, \omega, m) \in SO(3) \times \mathbb{R}^3 \times \mathbb{R}^2 : \det \bar{K}(C, \omega, m) = 0\}. \tag{53}$$

For fixed $t \in \mathbb{R}$, the set $\bar{\mathcal{F}}(t)$ is a hypersurface in $SO(3) \times \mathbb{R}^3 \times \mathbb{R}^2$. As in Section III B, given the significant variability of the Earth's magnetic field [21], it is very reasonable to make the following assumption:

Assumption 2 For any solution $(C_{bI}(t), \omega_{bI}(t), m_h(t)) \in SO(3) \times \mathbb{R}^3 \times \mathbb{R}^2$ of (3), (4) and (38) with (37), the set of times $\bar{\mathcal{T}} = \{t \in \mathbb{R} : (C_{bI}(t), \omega_{bI}(t), m_h(t)) \in \bar{\mathcal{F}}(t)\}$ has measure zero.

In a similar manner to Theorem 2 in Section III B, we obtain the following theorem

Theorem 3. Under Assumption 2, every solution $(C_{bI}(t), \omega_{bI}(t), m_h(t)) \in SO(3) \times \mathbb{R}^3 \times \mathbb{R}^2$ of (3), (4) and (38) with (37) is locally distinguishable under the measurement $s_b = C_{bI} s_I$ for almost all $t \in \mathbb{R}$.

IV. Numerical Examples - Attitude Determination of Passively Magnetically Stabilized Satellite

In this section, we consider the attitude determination of a passively magnetically stabilized satellite, with a single sun-vector measurement generated by

$$s_b(t_k)^m = C_{bI}(t_k) s_I(t_k) + v_k, \tag{54}$$

where v_k is zero-mean Gaussian with covariance $R_k = E\{v_k v_k^T\} = 3.04 \times 10^{-4}$ (generated using MATLAB's randn function).

The spacecraft attitude motion is described by the equations (3) and (4) with magnetic dipole moment given by (37).

The hysteresis rod magnetic dipole moments are given by

$$m_{hi} = b_{hi} V_{hi} / \mu_0, \;\; i = 1, 3, \tag{55}$$

where b_{hi} is the hysteresis rod magnetic flux density, V_{hi} the hysteresis rod volume, and $\mu_0 = 4\pi 10^{-7}$ H/m is the permeability of free space. The hysteresis rod magnetic flux densities obey the differential equations [22]

$$\dot{b}_{hi} = \frac{db_{hi}}{dh_i} \dot{h}_i, \;\; i = 1, 3, \tag{56}$$

where $h_i = e_i^T C_{bI} b_I/\mu_0$ is the component of the Earth's magnetic field strength vector along the spacecraft e_i axis. Finally,

$$\frac{db_{hi}}{dh_i} = \begin{cases} (2/\pi)k_i b_{mi} \cos^2\left(\pi b_{hi}/(2b_{mi})\right)\left((\bar{h}_i + h_{ci})/(2h_{ci})\right)^2, & \dot{h}_i \geq 0 \\ (2/\pi)k_i b_{mi} \cos^2\left(\pi b_{hi}/(2b_{mi})\right)\left((\bar{h}_i - h_{ci})/(2h_{ci})\right)^2, & \dot{h}_i < 0 \end{cases} \tag{57}$$

with $\bar{h}_i = h_i - (1/k_i)\tan\left(\pi b_{hi}/(2b_{mi})\right)$, for $i = 1, 3$, where b_{mi} is the hysteresis rod saturation, h_{ci} the hysteresis rod coercivity, and $k_i = 1/h_{ri}$ where h_{ri} is the hysteresis rod remanence.

When the hysteresis rods are appropriately sized, in steady-state the spacecraft attitude is such that the permanent magnet dipole is aligned with the Earth's magnetic field vector. As a result, since the hysteresis rod axes are perpendicular to the permanent magnet, their magnetic dipole moments tend towards zero. This appears to happen when the maximum hysteresis rod dipole moments (at saturation) are significantly smaller than the permanent magnet dipole moment. The paper [23] studies many existing on-orbit passively magnetically stabilized satellites, and demonstrates that when the hysteresis rods are too large (as they have been in some cases), they overwhelm the permanent magnets and the aforementioned steady-state attitude behaviour does not occur. In the next two subsections, we shall consider two scenarios; one with small hysteresis rods relative to the permanent magnets, and one with large hysteresis rods relative to the permanent magnets.

A. Small Hysteresis Rods

In this example, the satellite parameters from [24] are used. The spacecraft inertia matrix is given by $I = \text{diag}\{2.91058,\ 0.59261,\ 2.91058\} \times 10^{-2}$ kg·m^2. The permanent magnet dipole moment is $m_p = 3.0697$ A·m^2. The hysteresis rod parameters are $b_{mi} = 0.73$ T, $h_{ci} = 1.59$ A/m, $h_{ri} = 1.696$ A/m and $V_{hi} = 7.15 \times 10^{-8}$ m^3 for $i = 1, 3$. The maximum dipole moment for the hysteresis rods is $m_{h,\max} = 0.0415$ A·m^2, which is 1.4% of the permanent magnet dipole moment. The spacecraft is in a circular orbit with altitude 650 km, inclination 72 degrees, right ascension of the ascending node 100 degrees at epoch 1 February 2010. The Earth's magnetic field is computed using a 10^{th}

order IGRF model [21]. The spacecraft initial conditions are

$$C_{bI}(0) = \begin{bmatrix} -0.8881 & -0.4596 & 0 \\ 0.4407 & -0.8516 & 0.2839 \\ -0.1305 & 0.2521 & 0.9589 \end{bmatrix}, \ \omega_{bI}(0) = \begin{bmatrix} 0.05 \\ 0.05 \\ 0.05 \end{bmatrix} \text{ rad/s}, \ \ b_{hi}(0) = 0, \ \ i = 1, 3.$$

Figure 1 shows the resulting magnitude of the hysteresis rod magnetic flux densities. It can be seen

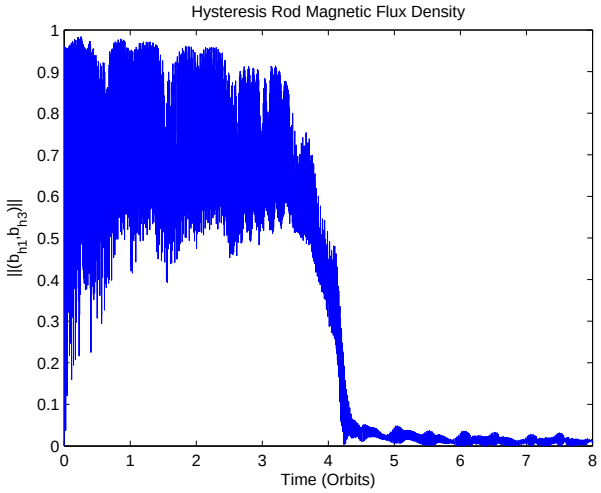

Fig. 1 Hysteresis Rod Magnetic Flux Density

that after approximately four orbits, the hysteresis rod magnetic flux densities reach a neighborhood of zero and stay there. This corresponds to the expected steady-state behaviour when the hysteresis rods are appropriately sized. Since the hysteresis rod dipole moments are significantly smaller than the permanent magnet dipole moment, they can be treated as disturbances from the point of view of state estimation scheme design. This is advantageous, since the hysteresis rod dynamics in (56) are discontinuous. Neglecting them yields continuously differentiable dynamics, for which an extended Kalman filter can be designed. Figure 2 examines the local distinguishability condition for this scenario, with plots of $\det K$ evaluated along the given solution, where K is given in (31). Note that for clarity, the columns of K have been normalized in the computation of the determinant. It is clear that Assumption 1 holds along the given solution. Hence, by Theorem 2 this justifies the development of an appropriate attitude estimation scheme.

Similar to [6] we formulate a multiplicative extended Kalman filter (MEKF) to solve this problem. Since formulation of MEKFs are standard [25], we simply summarize the final form of the filter

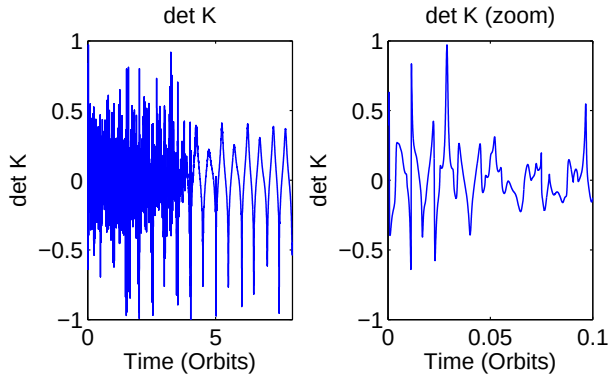

Fig. 2 Local Distinguishability Condition

here. The attitude estimation error is defined multiplicatively in a similar manner to (19) by

$$\exp(-p^{\times}) = C_{bI}(t)\hat{C}_{bI}(t)^T \tag{58}$$

for $p \in \mathbb{R}^3$, and the angular velocity estimation error is defined additively by

$$q = \omega_{bI}(t) - \hat{\omega}_{bI}(t). \tag{59}$$

Multiplicative Extended Kalman Filter

Given an initial unbiased estimate $(\hat{C}_{bI}(t_0)^+, \hat{\omega}_{bI}(t_0)^+)$ of $(C_{bI}(t_0), \omega_{bI}(t_0))$ with covariance $P(t_0)^+ = E\{[(p(t_0)^+)^T\ (q(t_0)^+)^T]^T[(p(t_0)^+)^T\ (q(t_0)^+)^T]\} \in \mathbb{R}^{6\times 6}$, and measurements $s_b(t_k)^m$, $k = 1, 2, 3, ...$, perform the recursion with $k = 1, 2, ...$:

1. Prediction step: integrate the equations

$$\dot{\hat{C}}_{bI}(t)^- = -(\hat{\omega}_{bI}(t)^-)^{\times}\hat{C}_{bI}(t)^-, \tag{60}$$

$$\dot{\hat{\omega}}_{bI}(t)^- = -(\hat{\omega}_{bI}(t)^-)^{\times}I\hat{\omega}_{bI}(t)^- + m_p e_2^{\times}\hat{C}_{bI}(t)^- b_I(t), \tag{61}$$

$$\dot{P}(t)^- = F(\hat{x}(t)^-)P(t)^- + P(t)^- F(\hat{x}(t)^-)^T + GQG^T, \tag{62}$$

over the interval $[t_{k-1}, t_k]$ with initial conditions $\hat{C}_{bI}(t_{k-1})^+, \hat{\omega}_{bI}(t_{k-1})^+$ and $P(t_{k-1})^+$, respectively, where

$$F(\hat{x}(t)^-) = \begin{bmatrix} -(\hat{\omega}_{bI}(t)^-)^{\times} & 1_3 \\ m_p I^{-1} e_2^{\times}\left(\hat{C}_{bI}(t)^- b_I(t)\right)^{\times} & I^{-1}\left((I\hat{\omega}_{bI}(t)^-)^{\times} - (\hat{\omega}_{bI}(t)^-)^{\times}I\right) \end{bmatrix}, \quad G = \begin{bmatrix} 0_{3\times 3} \\ I^{-1} \end{bmatrix}.$$

2. Correction step:

$$\begin{aligned}
\hat{C}_{bI}(t_k)^+ &= \exp\left[-\left(K_{p,k}\left(s_b(t_k)^m - \hat{C}_{bI}(t_k)^- s_I\right)\right)^\times\right]\hat{C}_{bI}(t_k)^-, \\
\hat{\omega}_{bI}(t_k)^+ &= \hat{\omega}_{bI}(t_k)^- + K_{\omega,k}\left(s_b(t_k)^m - \hat{C}_{bI}(t_k)^- s_I\right), \\
P(t_k)^+ &= \left(1_6 - K_k H\right) P(t_k)^- \left(1_6 - K_k H\right)^T + K_k R_k K_k^T.
\end{aligned}$$

where $H_k = \left[\begin{array}{cc} (\hat{C}_{bI}(t_k)^- s_I)^\times & 0_{3\times 3}\end{array}\right]$, and $K_k^T = \left[\begin{array}{cc} K_{p,k}^T & K_{\omega,k}^T\end{array}\right]^T = P(t_k)^- H_k^T \left(H_k P(t_k)^- H_k^T + R_k\right)^{-1}$.

In this example, the initial attitude and angular velocity estimates are given by $\hat{C}_{bI}(t_0)^+ = 1_3$ and $\hat{\omega}_{bI}(t_0)^+ = 0_{3\times 1}$, respectively. The initial state estimate covariance is given by $P(t_0)^+ = \text{diag}\{0.25 \cdot 1_3,\ 0.003 \cdot 1_3\}$, and the process noise covariance is given by $Q = 10^{-10} 1_3$. The sample period is taken to be $\Delta t = t_k - t_{k-1} = 1$ second. To concisely present the attitude and angular velocity estimation errors, the attitude estimation error is represented by the principal angle of rotation from the estimated attitude to the true attitude, given by [19, p. 13] $\phi = \|p\|_2$. The angular velocity estimation error is represented by $\|\omega_{bI} - \hat{\omega}_{bI}^+\|_2$.

Figure 3 shows the resulting transient attitude and angular velocity estimation errors. It can be seen that both converge rapidly. Table 1 shows the mean estimation errors computed over the periods from 1-3 orbits when the hysteresis rods are still very active (as shown in Figure 1), and 6-8 orbits when the hysteresis rods are almost inactive (as shown in Figure 1). As one would expect, the average estimation error is smaller once the satellite has converged to the steady-state attitude configuration. However, this shows that for a satellite with appropriately sized hysteresis rods (with much smaller capacity than the permanent magnets), reasonable attitude estimation, while treating hysteresis rod torques as disturbances, is still possible even before the steady-state attitude configuration has been reached.

Table 1 Mean Estimation Errors (Steady-State)

Period	ϕ_{av} (deg)	$\|\omega_{bI} - \hat{\omega}_{bI}^+\|_{2,av}$ (deg/s)
1–3 Orbits	1.0289	0.0634
6–8 Orbits	0.2167	0.0267

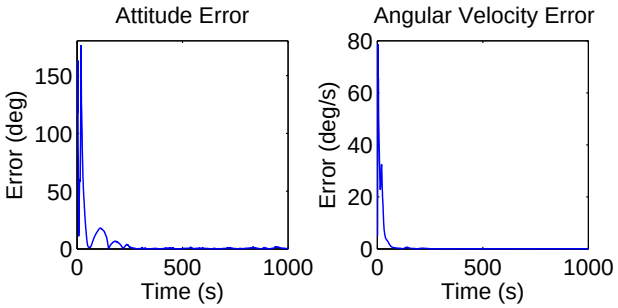

Fig. 3 Attitude and Angular Velocity Estimation Errors

B. Large Hysteresis Rods

We now present an example where the hysteresis rod magnitudes are significant compared to the permanent magnets.

The parameters used in the simulation are: spacecraft inertia matrix $I = \text{diag}\{0.14,\ 0.13,\ 0.145\}$ kg·m^2, permanent magnet dipole moment $m_p = 27.2$ A·m^2, hysteresis rod saturation $b_{mi} = 1.4$ T, hysteresis rod coercivity $h_{ci} = 2.8$ A/m, hysteresis rod remanence $h_{ri} = 1.7594$ A/m, hysteresis rod volume $V_{hi} = 1.4479 \times 10^{-5}$ m^3. The maximum dipole moment for the hysteresis rods is $m_{h,\max} = 16.1310$ A·m^2, which is 59.3% of the permanent magnet dipole moment. The spacecraft is in a circular orbit of altitude 650 km, with inclination $i = 98^o$ and right ascension of ascending node $\Omega = 100^o$ at epoch February 1, 2010. The Earth's magnetic field is once again generated using a 10^{th} order International Geomagnetic Reference Field (IGRF) model [21].

Figure 4 shows the resulting hysteresis rod magnetic flux densities, which both approach near constant values near saturation. This is significantly different steady-state attitude behaviour compared with the example in Section IV A. With such large hysteresis rods, it is no longer appropriate to treat them as disturbances for the purposes of state estimation. Indeed, implementation of the MEKF from the previous section to this spacecraft proved unsuccessful. Instead, the hysteresis rod parameters m_{h1} and m_{h3} must be included in the state vector and estimated also. We shall examine two methods of doing this. In the first, no knowledge of the hysteresis rod parameters is assumed, but takes advantage of the hysteresis rod steady-state behaviour. In the second, knowledge of the hysteresis rod parameters is assumed.

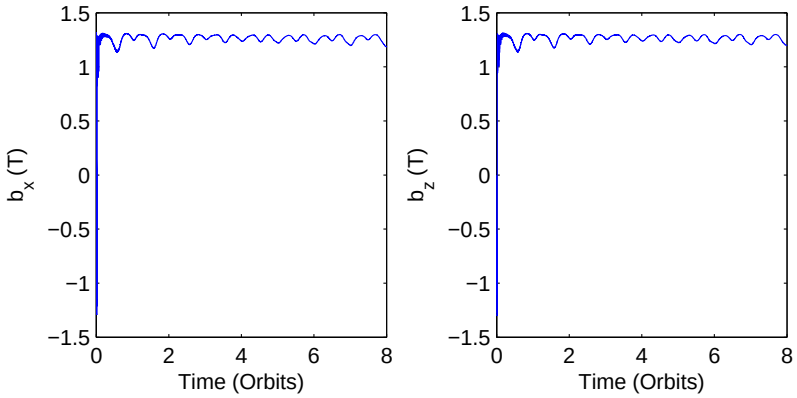

Fig. 4 Hysteresis Rod Magnetic Flux Densities

1. No Knowledge of Hysteresis Rod Parameters

In the case of no knowledge of the hysteresis rod parameters, we take advantage of their near constant steady-state behaviour. As such, for the purpose of state estimation, we treat the hysteresis rod dipole moments as unknown constant values to be estimated, as in Section III C. Figure 5 examines the local distinguishability condition for this scenario, with plots of $\det \bar{K}$ evaluated along the given solution, where $\bar{K}$ is given in (52). Note that for clarity, the columns of $\bar{K}$ have been normalized in the computation of the determinant. It is clear that Assumption 2 holds along the given solution. Hence, by Theorem 3 this justifies the development of an appropriate attitude estimation scheme. In addition to the attitude and angular velocity estimation errors defined in

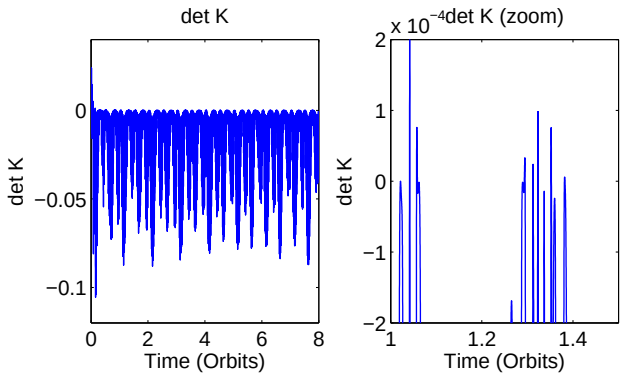

Fig. 5 Local Distinguishability Condition

(58) and (59), define the additive hysteresis rod dipole moment estimation error as

$$r = m_h(t) - \hat{m}_h(t). \tag{63}$$

The multiplicative extended Kalman filter from Section IV A is now modified to include the hysteresis rod dipole moments as follows.

Multiplicative Extended Kalman Filter

Given an initial unbiased estimate $(\hat{C}_{bI}(t_0)^+, \hat{\omega}_{bI}(t_0)^+, \hat{m}_h(t_0)^+)$ of $(C_{bI}(t_0), \omega_{bI}(t_0), m_h(t_0))$ with covariance $P(t_0)^+ = E\{[(p(t_0)^+)^T\ (q(t_0)^+)^T\ r(t_0)^+]^T[(p(t_0)^+)^T\ (q(t_0)^+)^T\ (r(t_0)^+)^T]\} \in \mathbb{R}^{8\times 8}$, and measurements $s_b(t_k)^m$, $k = 1, 2, 3, ...$, perform the recursion with $k = 1, 2, ...$:

1. Prediction step: set $\hat{m}_h(t_k)^- = \hat{m}_h(t_{k-1})^+$ and integrate the equations (60), (61) and (62) over the interval $[t_{k-1}, t_k]$ with initial conditions $\hat{C}_{bI}(t_{k-1})^+, \hat{\omega}_{bI}(t_{k-1})^+$ and $P(t_{k-1})^+$, respectively, where $\hat{b}_b(t)^- = \hat{C}_{bI}(t)^- b_I(t)$, $\hat{m}_b(t_{k-1})^+ = m_p e_2 + [e_1\ e_3]\hat{m}_h(t_{k-1})^+$,

$$F(\hat{x}^-(t)) = \begin{bmatrix} -(\hat{\omega}_{bI}(t)^-)^\times & 1_3 & 0_{3\times 3} \\ I^{-1}(\hat{m}_b(t_{k-1})^+)^\times(\hat{b}_b(t)^-)^\times & I^{-1}\left((I\hat{\omega}_{bI}(t)^-)^\times - (\hat{\omega}_{bI}(t)^-)^\times I\right) & -I^{-1}(\hat{b}_b(t)^-)^\times[e_1\ e_3] \\ 0_{2\times 3} & 0_{2\times 3} & 0_{2\times 2} \end{bmatrix},$$

$$G = \begin{bmatrix} 0_{3\times 3} & 0_{3\times 2} \\ I^{-1} & 0_{3\times 2} \\ 0_{2\times 3} & 1_2 \end{bmatrix}.$$

2. Correction step:

$$\begin{aligned} \hat{C}_{bI}(t_k)^+ &= \exp\left[-\left(K_{p,k}\left(s_b(t_k)^m - \hat{C}_{bI}(t_k)^- s_I\right)\right)^\times\right]\hat{C}_{bI}(t_k)^-, \\ \hat{\omega}_{bI}(t_k)^+ &= \hat{\omega}_{bI}(t_k)^- + K_{\omega,k}\left(s_b(t_k)^m - \hat{C}_{bI}(t_k)^- s_I\right), \\ \hat{m}_k(t_k)^+ &= \hat{m}_h(t_k)^- + K_{m,k}\left(s_b(t_k)^m - \hat{C}_{bI}(t_k)^- s_I\right), \\ P(t_k)^+ &= (1_8 - K_k H)\,P(t_k)^-\,(1_8 - K_k H)^T + K_k R_k K_k^T. \end{aligned}$$

where $H_k = \begin{bmatrix} (\hat{C}_{bI}(t_k)^- s_I)^\times & 0_{3\times 3} & 0_{3\times 2} \end{bmatrix}$, and $K_k^T = \begin{bmatrix} K_{p,k}^T & K_{\omega,k}^T & K_{\omega,k}^T \end{bmatrix}^T = P(t_k)^- H_k^T\left(H_k P(t_k)^- H_k^T + R_k\right)^{-1}$.

In this example, the initial attitude and angular velocity estimates are given by $\hat{C}_{bI}(t_0)^+ = 1_3$, $\hat{\omega}_{bI}(t_0)^+ = 0_{3\times 1}$ and $\hat{m}_h(t_0)^+ = 0_{2\times 1}$, respectively. The initial state estimate covariance is given

by $P(t_0)^+ = \text{diag}\{0.25 \cdot 1_3,\ 0.003 \cdot 1_3,\ 100 \cdot 1_2\}$, and the process noise covariance is given by $Q = \text{diag}\{10^{-10}1_3,\ 10^{-2}1_2\}$. The sample period is taken to be $\Delta t = t_k - t_{k-1} = 1$ second. The filter is applied from $t_0 = 2000$ seconds (approximately 1/3 orbit) onwards, since as shown in Figure 4, the hysteresis rod flux densities have reached their steady-state condition by this time.

Figure 6 shows the resulting transient estimation errors. It can be seen that they converge rapidly. Table 2 shows the mean estimation errors at steady-state. Compared with the steady-state estimation errors in Table 1, when hysteresis rods are neglected, it can be seen that a significant improvement in performance can result from simply estimating the hysteresis rod dipole moments as if they are constant.

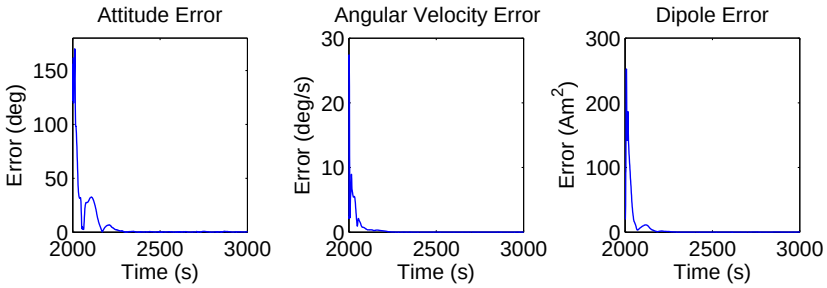

Fig. 6 Attitude, Angular Velocity and Magnetic Dipole Moment Estimation Errors

Table 2 Mean Estimation Errors (Steady-State)

ϕ_{av} (deg)	$\|\omega_{bI} - \hat{\omega}_{bI}^+\|_{2,av}$ (deg/s)	$\|m_h - \hat{m}_h^+\|_{2,av}$ (A·m^2)
0.1265	0.0108	0.0671

2. Knowledge of Hysteresis Rod Parameters

If the hysteresis rod parameters are known, then the hysteresis rod dynamics may be incorporated into a state estimation scheme to further improve state estimation performance. Since the hysteresis rod dynamics in (56) are discontinuous, this precludes the use of any type of extended Kalman filter. Instead, a sigma point filter is used here. Specifically, the cubature Kalman filter from [16] is used in this example. To keep the dimension of the state vector small, the spacecraft attitude is represented by the unit quaternion $p = [\epsilon^T\ \eta]^T$ where ϵ and η are the vector and scalar

components of the quaternion, respectively with [19, pp. 17–18]

$$C_{bI}(p) = (\eta^2 - \epsilon^T\epsilon)1_3 + 2\epsilon\epsilon^T - 2\eta\epsilon^\times. \tag{64}$$

Correspondingly, the kinematics in (3) are replaced by their quaternion equivalent [19, p. 26]

$$\begin{aligned} \dot{\epsilon} &= \tfrac{1}{2}(\epsilon^\times + \eta 1_3)\omega_{bI}, \\ \dot{\eta} &= -\tfrac{1}{2}\epsilon^T\omega_{bI}, \end{aligned} \tag{65}$$

Defining the state vector

$$x = \begin{bmatrix} \epsilon^T & \eta & \omega_{bI}^T & b_{h1} & b_{h3} \end{bmatrix}^T, \tag{66}$$

for state estimation purposes we consider the system

$$\dot{x} = f(x,t) + Gw, \tag{67}$$

$$y_k = c(x(t_k)) + v_k, \tag{68}$$

where $f(x,t)$ is determined by the right-hand sides of (65), (4) and (56), $w \in \mathbb{R}^5$ is a zero-mean white noise process with covariance Q,

$$G = \begin{bmatrix} 0_{4\times 3} & 0_{4\times 2} \\ I^{-1} & 0_{3\times 2} \\ 0_{2\times 3} & 1_2 \end{bmatrix},$$

and the measurement function $c(x)$ is obtained from the quaternion equivalent of (54), and is given by $c(x) = C_{bI}(p)s_I$, where $C_{bI}(p)$ is given in (64). A complicating factor in this example is that the quaternion estimate $\hat{p}$ is required to satisfy a unit length constraint $\|\hat{p}\|_2 = 1$. In addition, the hysteresis rod magnetic flux densities must satisfy the constraints [22]

$$\hat{b}_{hi} \geq b_{mi}(2/\pi)\tan^{-1}\left(k_i(\hat{h}_i - h_{ci})\right) \tag{69}$$

$$\hat{b}_{hi} \leq b_{mi}(2/\pi)\tan^{-1}\left(k_i(\hat{h}_i + h_{ci})\right), \tag{70}$$

for $i = 1, 3$. Accordingly, following the approach in [26], the quaternion estimate $\hat{p}(t_k)^+$ is renormalized at each time step after the Kalman correction, and the hysteresis rod magnetic flux density estimates $\hat{b}_{hi}(t_k)^+$ are then scaled such that the constraints in (69) and (70) are satisfied. Similar to [26], a second order correction term is then added to the posterior covariance. The

cubature Kalman filter applied in this example is summarized as follows.

Cubature Kalman Filter

Given $\hat{x}(t_0)^+$, $P(t_0)^+ = E\{(x(t_0) - \hat{x}(t_0)^+)(x(t_0) - \hat{x}(t_0)^+)^T\}$, and measurements y_k, k=1,2,.... perform the recursion with $k = 1, 2, ...$:

1. Compute the Cholesky decomposition $S(t_{k-1})^+ = \text{chol}(P(t_{k-1})^+)$, and compute the cubature points

$$\begin{aligned}\mathcal{X}_i(t_{k-1})^+ &= \hat{x}(t_{k-1})^+ + 3S(t_{k-1})_i^+, \ i = 1, ..., 9,\\ \mathcal{X}_{i+9}(t_{k-1})^+ &= \hat{x}(t_{k-1})^+ - 3S(t_{k-1})_i^+, \ i = 1, ..., 9.\end{aligned}$$

2. Let $\delta t = (t_k - t_{k-1})/\ell$, for some positive integer ℓ. For $j = 1$, set $\mathcal{X}_i(t_{k-1} + (j-1)\delta t)^- = \mathcal{X}_i(t_{k-1})^+$. For $j = 1, ..., \ell$, perform the recursion:

   (a) Numerically integrate $\dot{x} = f(x, t)$ from $t_{k-1}+(j-1)\delta t$ to $t_{k-1}+j\delta t$ with initial conditions corresponding to each of the previous cubature points $\mathcal{X}_i(t_{k-1} + (q-1)\delta t)^-$ to obtain $\mathcal{X}_i(t_{k-1} + j\delta t)^-$.

   (b) Update the covariance $P(t_{k-1} + j\delta t)^-$ according to

$$P(t_{k-1} + j\delta t)^- = \delta t G Q G^T$$
$$+\tfrac{1}{18}\textstyle\sum_{i=1}^{18}(\mathcal{X}_i(t_{k-1} + j\delta t)^- - \hat{x}(t_{k-1} + j\delta t)^-)(\mathcal{X}_i(t_{k-1} + j\delta t)^- - \hat{x}(t_{k-1} + j\delta t)^-)^T,$$

   where $\hat{x}(t_{k-1} + j\delta t)^- = (1/18)\sum_{i=1}^{18}\mathcal{X}_i(t_{k-1} + j\delta t)$.

   (c) Compute $S(t_{k-1} + j\delta t)^- = \text{chol}(P(t_{k-1} + j\delta t)^-)$, and compute new cubature points

$$\begin{aligned}\mathcal{X}_i(t_{k-1} + j\delta t)^- &= \hat{x}(t_{k-1} + j\delta t)^- + 3S(t_{k-1} + j\delta t)_i^+, \ i = 1, ..., 0,\\ \mathcal{X}_{i+9}(t_{k-1} + j\delta t)^- &= \hat{x}(t_{k-1} + j\delta t)^- - 3S(t_{k-1} + j\delta t)_i^+, \ i = 1, ..., 9.\end{aligned}$$

3. Transform the cubature points to obtain $\mathcal{Y}_{k,i} = c(\mathcal{X}_i(t_k)^-)$ for $i = 1, ..., 18$, and compute the conditional expectation $\hat{y}_k^- = \frac{1}{18}\sum_{i=1}^{18}\mathcal{Y}_{k,i}$ and covariances

$$\begin{aligned}P_{yy}(t_k)^- &= \frac{1}{18}\sum_{i=1}^{18}(\mathcal{Y}_{k,i} - \hat{y}_k^-)(\mathcal{Y}_{k,i} - \hat{y}_k^-)^T + R_k,\\ P_{xy}(t_k)^- &= \frac{1}{18}\sum_{i=1}^{18}(\mathcal{X}_i(t_k)^- - \hat{x}(t_k)^-)(\mathcal{Y}_{k,i} - \hat{y}_k^-)^T.\end{aligned}$$

4. Set $K_k = P_{xy}(t_k)^-(P_{yy}(t_k)^-)^{-1}$, and compute the unconstrained corrections

$$\begin{aligned}\hat{x}_u(t_k)^+ &= \hat{x}(t_k)^- + K_k(y_k - \hat{y}_k^-),\\ P_u(t_k)^+ &= P(t_k)^- - K_k P_{yy}(t_k)^- K_k^T.\end{aligned}$$

5. With $\hat{x}_u = [\hat{p}_u^T\ \hat{\omega}_{bI,u}^T\ \hat{p}_{h1,u}\ \hat{p}_{h3,u}]^T$, set $\hat{p}(t_k)^+ = \hat{p}_u(t_k)^+/\|\hat{p}_u(t_k)^+\|_2$, $\hat{\omega}_{bI}(t_k)^+ = \hat{\omega}_{bI,u}(t_k)^+$, and for $i = 1, 3$, set

$$\hat{b}_{hi}(t_k)^+ = \begin{cases} b_{il}, & \text{if } \hat{b}_{hi,u}(t_k)^+ < b_{il},\\ b_{iu}, & \text{if } \hat{b}_{hi,u}(t_k)^+ > b_{iu},\\ \hat{b}_{hi,u}(t_k)^+, & \text{otherwise,}\end{cases}$$

and $P(t_k)^+ = P_u(t_k)^+ + (1/\tilde{r})(\hat{x}(t_k)^+ - \hat{x}_u(t_k)^+)(\hat{x}(t_k)^+ - \hat{x}_u(t_k)^+)^T$, where $b_{il} = b_{mi}(2/\pi)\tan^{-1}\left(k_i(\hat{h}_i - h_{ci})\right)$, $b_{iu} = b_{mi}(2/\pi)\tan^{-1}\left(k_i(\hat{h}_i + h_{ci})\right)$, $\hat{h}_i = e_i^T C_{bI}(\hat{p}(t_k)^+)b_I(t_k)/\mu_0$ and $\tilde{r} = (y_k - \hat{y}_k^-)^T\left(P_{yy}(t_k)^-\right)^{-1}(y_k - \hat{y}_k^-)$.

Note that the recursion within Step 2 above is formulated to approximate the continuous propagation of the process dynamics and covariance (the system in (68) is continuous).

The initial estimates are $\hat{q}(t_0)^+ = [0\ 0\ 0\ 1]^T$, $\hat{\omega}_{bI}(t_0)^+ = [0\ 0\ 0]^T$, $\hat{b}_{h1}(t_0)^+ = \hat{b}_{h3}(t_0)^+ = 0$, and the initial estimate error covariance is taken to be $P(t_0)^+ = \text{diag}\{0.25 \cdot 1_4,\ 0.003 \cdot 1_3,\ 1_2\}$. The process noise covariance is taken to be $Q = \text{diag}\{10^{-10} \cdot 1_3,\ 10^{-8} \cdot 1_2\}$. The sample period is $\Delta t = t_k - t_{k-1} = 1$ second, and the propagation step is divided into $\ell = 10$ sub-intervals.

To maintain consistency with the previous two numerical examples, the attitude estimation error is represented by the principal angle of rotation from the true attitude to the estimated attitude, given by $\phi = \cos^{-1}\left((\text{trace}[C_{bI}(\hat{p})C_{bI}^T(p)] - 1)/2\right)$ [19, p. 13].

Figure 7 shows the resulting estimation errors. It can be seen that the estimation errors converge to small values within 400 seconds, despite the large initial estimation errors. Table 3 shows the resulting mean steady-state estimation errors. Compared with Table 2 for the MEKF where the hysteresis rod dipoles are treated as constant, it can be seen that the state estimation scheme performs significantly better when hysteresis rods dynamics are incorporated.

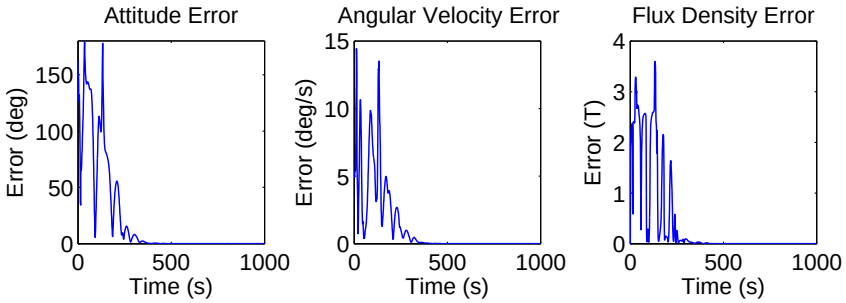

Fig. 7 Attitude, Angular Velocity and Magnetic Flux Density Estimation Errors

Table 3 Mean Estimation Errors (Steady-State)

ϕ_{av} (deg)	$\|\omega_{bI} - \hat{\omega}_{bI}^{+}\|_{2,av}$ (deg/s)	$\|(b_{h1}, b_{h3}) - (\hat{b}_{h1}^{+}, \hat{b}_{h3}^{+})\|_{2,av}$ (T)
0.0546	0.0040	1.53×10^{-4}

V. Conclusions

This paper has considered attitude estimation for passively magnetically stabilized spacecraft using only sun vector measurements. It was demonstrated with numerical examples, that for passively stabilized spacecraft using permanent magnets and magnetic hysteresis rods, the hysteresis rod dipole moments tend to near constant steady-state values. Correspondingly, analytical investigations of local observability have been performed by treating the spacecraft magnetic dipole moment as constant for two cases. In the first case, it is assumed that the dipole moment is fully known. Such a scenario occurs when the hysteresis rod dipole moments are insignificant compared with the permanent magnets. It has been shown that under reasonable assumptions on the Earth's magnetic field, the spacecraft attitude and angular velocity are observable from a sun vector measurement alone. In the second case, it is assumed that one component of the dipole moment is known, but that the remaining two need to be estimated. Such a scenario occurs at steady-state when the hysteresis rod dipole moments are significant compared with the permanent magnets. It has been shown that again under reasonable assumptions on the Earth's magnetic field, the spacecraft attitude, angular velocity and the unknown part of the dipole moment are observable from a sun vector measurement alone. Motivated by these results, three state estimation schemes using sun-vector measurements only have been formulated for the estimation of spacecraft attitude, angular velocity

and the hysteresis rod dipole moments. Numerical examples demonstrate that these schemes are very effective.

VI. Acknowledgements

This research was supported by a Natural Sciences and Engineering Research Council of Canada Engage grant.

References

[1] Bar-Itzhack, I. Y. and Reiner, J., "Recursive Attitude Determination from Vector Observations: Direction Cosine Matrix Identification," *AIAA Journal of Guidance*, Vol. 7, No. 1, 1984, pp. 51–56. Doi: 10.2514/3.56362.

[2] Choukroun, D., Weiss, H., Bar-Itzhack, I. Y., and Oshman, Y., "Direction Cosine Matrix Estimation from Vector Observations using a Matrix Kalman Filter," *IEEE Transactions on Aerospace and Electronic Systems*, Vol. 46, No. 1, 2010, pp. 61–79. Doi: 10.1109/TAES.2010.5417148.

[3] Grip, H. F., Fossen, T. I., Johansen, T. A., and Saberi, A., "Attitude Estimation Using Biased Gyro and Vector Measurements With Time-Varying Reference Vectors," *IEEE Transactions on Automatic Control*, Vol. 57, No. 5, 2012, pp. 1332–1338. Doi: 10.1109/TAC.2011.2173415.

[4] Trumpf, J., Mahony, R., Hamel, T., and Lageman, C., "Analysis of Non-Linear Attitude Observers for Time-Varying Reference Measurements," *IEEE Transactions on Automatic Control*, Vol. 57, No. 11, 2012, pp. 2789–2800. Doi: 10.1109/TAC.2012.2195809.

[5] Crassidis, J. L., Markley, F. L., and Cheng, Y., "Survey of Nonlinear Attitude Estimation Methods," *AIAA Journal of Guidance, Control, and Dynamics*, Vol. 30, No. 1, 2007, pp. 12–28. Doi: 10.2514/1.22452.

[6] Burton, R., Rock, S., Springmann, J., and Cutler, J., "Online Attitude Determination of a Passively Magnetically Stabilized Spacecraft," in "Proceedings of the 23rd AAS/AIAA Space Flight Mechanics Meeting," Kauai, Hawaii, 2013. AAS 13-364.

[7] Akella, M. R., Seo, D., and Zanetti, R., "Attracting Manifolds for Attitude Estimation in Flatland and Otherlands," *Journal of the Astronautical Sciences*, Vol. 54, No. 3-4, 2006, pp. 635–655. Doi: 10.1007/BF03256510.

[8] Khosravian, A. and Namvar, M., "Rigid Body Attitude Control Using a Single Vector Measurement and Gyro," *IEEE Transactions on Automatic Control*, Vol. 57, No. 5, 2012, pp. 1273–1279. Doi: 10.1109/TAC.2011.2174663.

[9] Psiaki, M. L., Martel, F., and Pal, P. K., "Three-Axis Attitude Determination via Kalman Filtering of Magnetometer Data," *AIAA Journal of Guidance*, Vol. 13, No. 3, 1990, pp. 506–514. Doi: 10.2514/3.25364.

[10] Psiaki, M. L., Martel, F., and Pal, P. K., "Global Magnetometer-Based Spacecraft Attitude and Rate Estimation," *AIAA Journal of Guidance, Control and Dynamics*, Vol. 27, No. 2, 2004, pp. 240–250. Doi: 10.2514/1.1039.

[11] Pong, C. M., "High-Precision Pointing and Attitude Estimation and Control Algorithms for Hardware-Constrained Spacecraft," *Doctoral Thesis, Massachussetts Institute of Technology, 2014*.

[12] Oshman, Y. and Dellus, F., "Spacecraft Angular Velocity Estimation Using Sequential Observations of a Single Directional Vector," *AIAA Journal of Spacecraft and Rockets*, Vol. 40, No. 2, 2003, pp. 237–247. Doi: 10.2514/2.3938.

[13] Tortora, P., Oshman, Y., and Santoni, F., "Attitude Independent Estimation of Spacecraft Angular Rate Using Geomagnetic Field Observations," in "Proceedings of the IEEE Aerospace Conference," Big Sky, MT, March 2003, 2003, pp. 2637–2645.

[14] Psiaki, M. L. and Oshman, Y., "Spacecraft Attitude Rate Estimation from Geomagnetic Field Measurements," *AIAA Journal of Guidance, Control and Dynamics*, Vol. 26, No. 2, 2003, pp. 244–252. Doi: 10.2514/2.5065.

[15] Burton, R., Rock, S., Springmann, J., and Cutler, J., "Dual Attitude and Parameter Estimation of Passively Magnetically Stabilized Spacecraft," in "Proceedings of the 63rd International Astronautical Congress," Naples, Italy, 2012. IAC-12-C1.9.6.

[16] Arasaratnam, I. and Haykin, S., "Cubature Kalman Filters," *IEEE Transactions on Automatic Control*, Vol. 54, No. 6, 2009, pp. 1254–1269. Doi: 10.1109/TAC.2009.2019800.

[17] Khalil, H. K., *Nonlinear Systems*, Prentice Hall, Upper Saddle River, New Jersey, 3rd ed., 2002. Pp. 88-89, 102-103.

[18] Isidori, A., *Nonlinear Control Systems*, Springer, London, 3rd ed., 1995. P. 472.

[19] Hughes, P. C., *Spacecraft Attitude Dynamics*, Dover, Mineola, New York, 2nd ed., 2004.

[20] de Ruiter, A. H. J., Damaren, C. J., and Forbes, J. R., *Spacecraft Dynamics and Control: An Introduction*, John Wiley and Sons Ltd., West Sussex, United Kingdom, 2013. Pp. 59-60.

[21] Wertz, J. R., *Spacecraft Attitude Determination and Control*, Kluwer Academic Publishers, Dordrecht, The Netherlands, 1978. App. H.

[22] Burton, R., Stareky, J., and Rock, S., "A New Method for Simulating the Attitude Dynamics of a Passively Magnetically Stabilized Spacecraft," in "Proceedings of the 22nd AAS/AIAA Space Flight

Mechanics Meeting," Charleston SC, 2012. AAS 12-169.

[23] Rawashdeh, S. A. and Lumpp, J. E., "Nano-Satellite Passive Attitude Stabilization Systems Design by Orbital Environment Modeling and Simulation," in "Proceedings of the AIAA Infotech@Aerospace Conference," Atlanta, Georgia, 2010. AIAA 2010-3413.

[24] Park, G., Seagraves, S., and McClamroch, N. H., "A Dynamic Model of a Passive Magnetic Attitude Control System for the RAX Nanosatellite," in "Proceedings of the AIAA Guidance, Navigation and Control Conference," Toronto, Canada, 2010. AIAA 2010-8154.

[25] Markley, F. L., "Attitude Error Representations for Kalman Filtering," *AIAA Journal of Guidance, Control and Dynamics*, Vol. 26, No. 2, 2003, pp. 311–317. Doi: 10.2514/2.5048.

[26] Zanetti, R., Majji, M., Bishop, R. H., and Mortari, D., "Norm-Constrained Kalman Filtering," *AIAA Journal of Guidance, Control, and Dynamics*, Vol. 32, No. 5, 2009, pp. 1458–1465. Doi: 10.2514/1.43119.